Transactions of the Korean Nuclear Society Spring Meeting
Jeju, Korea, May 29-30, 2014

Oxidation and Explosion Characteristics of Nuclear Graphite Powder

Eung-Seon Kim[a*], Min-Hwan Kim[a], Yong-Wan Kim[a], Yi-Hyun Park[b], Seung-Yon Cho[b]
[a]*Korea Atomic Energy Research Institute, 989-111 Daedeok-daero, Yuseong-gu, Daejeon, 305-353*
[b]*National Fusion Research Institute, 169-148, Gwahangno, Yuseong-gu, Daejeon 305-806*
[*]*Corresponding author: kimes@kaeri.re.kr*

1. Introduction

In a high temperature gas-cooled reactor, nuclear graphite has been widely used as the fuel element, moderator or reflector blocks and core support structures owing to its excellent moderating power, mechanical properties, and machinability [1]. For the same reason, it will be used in a helium cooled ceramic reflector test blanket module for an ITER [2]. Each sub-module has a seven-layer breeding zone: three neutron multiplier layers packed with beryllium pebbles, three lithium ceramic pebble packed tritium breeder layers, and a reflector layer packed with 1 mm diameter graphite pebbles to reduce the volume of beryllium. The abrasion of graphite structures due to the relative motion or thermal cycle during operation may produce graphite dust [3, 4]. It is thought that the graphite dust is more oxidative than bulk graphite, and thus oxidation behavior of graphite dust must be examined to analyze the safety of the reactors during an air ingress accident. In this study, the oxidation and explosion behaviors of ball-milled nuclear graphite powder were investigated.

2. Methods and Results

The material used in this study was a high purity, super fine-grained isotropic nuclear grade graphite, IG-110, made by Toyo Tanso Co. Ltd. Japan. The graphite blocks were initially crushed with a jaw crusher and then ground with a mortar grinder. The ball milling was performed on a planetary mill set at 400 rev/min for 10, 20, 30, 60, 300, 600, and 1200 minutes. With a ball-to-weight ratio of 20, 40 grams of the grinded powder and hardened steel balls (8.0 mm in diameter) were sealed under an argon atmosphere in a hardened steel vial. The milled powders were taken out and put into bottles in a glove box filled with argon gas, and the loosely capped bottles were then kept in the atmosphere.

The particle size distribution was meaured using a laser scattering particle size distribution analyzer (Horiba, LA950). The Brunauer-Emmet-Teller (BET) surface area was measured through multipoint nitrogen adsorption (Micromeritics, ASAP 2420) after pretreatment at 120 ^{o}C for 2 hr. Raman spectroscopy was measured at room temperature in an ambient atmosphere using a Jobin-Yvon LabRam HR with a LN_2 cooled CCD multichannel detector in a conventional backscattering geometry. The spectra were excited with the 514.5 nm line of an Ar-ion laser. The laser beam power was 2 mW and the Raman parameters of the spectrum peaks were obtained by Lorentzian fitting.

Thermogravometric and differential scanning calorymetric analyses (TG-DSC) were perfomed in air using a Setaram DTA, GA 92-18 at a heating rate of 10 ^{o}C min^{-1} for up to 900 ^{o}C. Explosion tests were performed using a standard 20-L apparatus.

3. Results and Discussion

Fig. 1 shows the changes in the mean particle size on the BET surface area with the milling time. The initial 10 min of milling led primarily to a size reduction by a fracture of the larger particles. However, the particle size increased after milling for 30 min and then decreased up to 300 min. Once again, the particle size increased slightly but remained nearly steady after 1000 min. Equilibrium between breakage and rewelding, or agglomeration of particles during milling, will lead to this behaviour [5]. The specific surface area increased linealy up to 60 min (528 m^2/g), but abruptly decreased after 300 min (332 m^2/g), and then gradually decreased until 1200 min (267 m^2/g). The formation of small particles is the major reason for the increased external surface area. The lower BET surface area after 300 min can result from the presence of CO_2 monolayers, which were not removed during the pretreatment step [6].

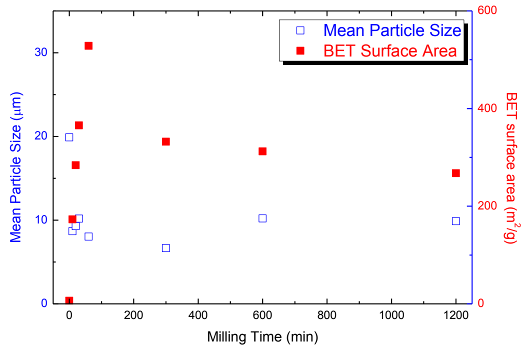

Fig. 1. Changes in particle size and BET surface area.

Fig. 2 shows the change in aman spectra with the milling time. The Raman spectrum of the as-gound powder shows an intense graphite peak at 1580 cm^{-1} (G peak) in addition to a very weak disordered peak at 1350 cm^{-1} (D peak) [7]. The milled powder exhibits an intense D peak stronger than the G peak. Both the D and G peaks broaden continuously with the milling time. According to Tuinstra and Koening [8], the relative intensity ratio of two peaks, $R = I_D/I_G$ is known to be inversely proportional to the in-plane crystalline size (L_a) of graphite by the empirical relation $L_a = C/R$, where C is 4.4 nm. Fig. 3 shows a decrease in the graphite crystal size. It is well known that the fraction of active edge sites increases with a decrease in the crystallite size, L_a.

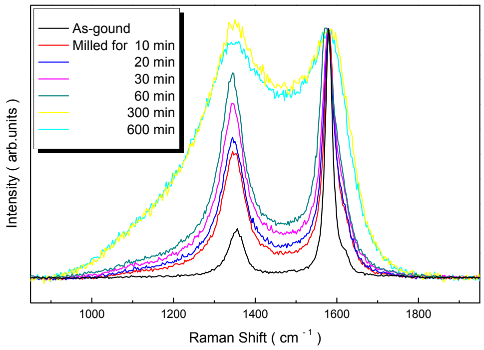

Fig. 2. Change in Raman spectra of ball milled graphite.

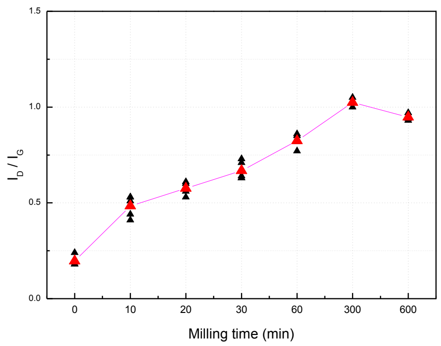

Fig. 3. Change in I_D/I_G of ball milled graphite.

In the as-gound powder, the heat flow owing to an exothermic oxidation reaction began to increase linealy at 726 ^{o}C, while the weight decreased proportionally. In the milled powders, the reaction heat was detected at 122 ^{o}C with minimal weight loss, and the temperature where the bulk oxidation begins to occur decreased, i.e., 600 ^{o}C for the 30 min powder, and 400 ^{o}C for the 600 min powder.

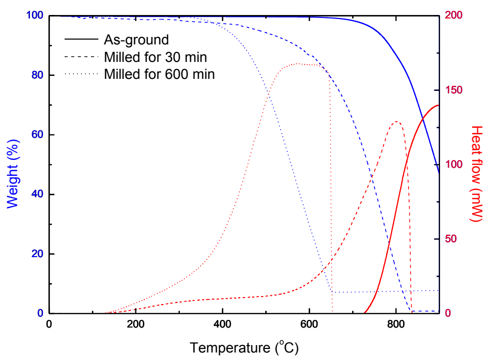

Fig. 4. Change in TG-DSC curve

As shown in Fig. 4, the maximum overpressures and pressure rise rates of the as-ground powder were 6.1 bar and 98.5 bar/sec, respectively. However, after the 300 min milling, the maximum overpressures and pressure rise rates increased to 8.9 bar and 555 bar/sec, respectively. Also, the lower explosion concentration limit (LEL) significantly decreased from 250 g/cm^3 to 30 g/cm^3. The explosion indices of the 300 min powder are much higher than the previously reported values [10].

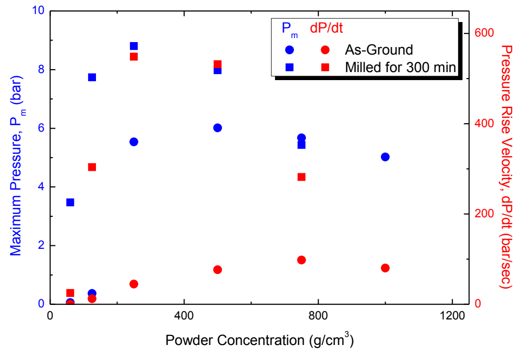

Fig. 5. Change in explosion parameters, P_m and dP/dt.

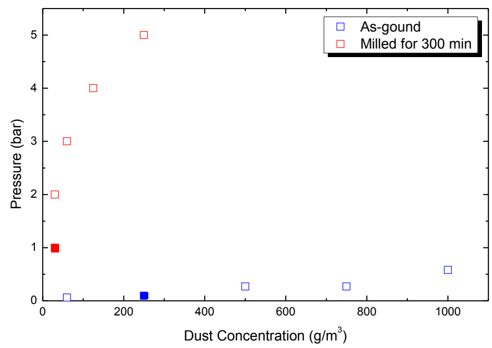

Fig. 6. Change in lower explosion concentration.

According to previous work, the abrupt decrease in the BET surface area of the 300 min powder is attributed to the chemisorption of oxygen on an activated surface after exposure to air. Accordingly, it is reasonable to assume that the weight loss and heat flow at low temperature is attributed to the presence of absorbed CO_2 [11]. The increase in chemical reactivity after the ball milling is caused not only by increasing the specific surface area but also by growing disorder on an atomic scale [12]. Distortion and topological rearrangement of sp2 bonds in the sence of two-dimensional random networks play an essential role in the enhancement of the chemical reactivity of nano-sized carbon powder.

3. Conclusions

An examination was made to characterize the oxidation behavior of ball-milled nuclear graphite powder through a TG-DSC analysis. With the ball milling time, the BET surface area increased with a reduction of the particle size, but decreased with the chemisorption of O_2 on the activated surface. The enhancement of the oxidation after the ball milling is attributed to both increases in the specific surface area and atomic scale defects in the graphite structure.

Acknowledgement

This study was supported by Nuclear Research & Development Program of the National Research Foundation of Korea (NRF) grant funded by the Korean government (MSIP) (Grant code: NRF-2012M2A8A2025682, NFRI-IN1303).

REFERENCES

[1] T. D. Burchell (eds.): 'Carbon materials for advanced technologies'; 1999, Oak Ridge, Pergamon.
[2] S. Cho, M. Y. Ahn, D. H. Kim, E. S. Lee, S. Yun, N. Z. Cho: 'Current status of design and analysis of Korean helium-cooled solid breeder test blanket module', Fusion Eng. Des., 2008, **83**, 1163-1168.
[3] M. Rostamian, S. Arifeen, G. P. Potirniche and A. Tokuhiro: 'Initial prediction of dust production in pebble bed reactors', Mech. Sci., 2011, **2**, 189-195
[4] A. Denkevits and S. Dorofeev: 'Dust explosion hazard in ITER: Explosion indices of fine graphite and tungsten dusts and their mixtures', Fusion Eng. Des., 2005**, 75-79**, 1135-1139.
[5] N.J. Welham, J.S. Williams: 'Extended Milling of Graphite and Activated Carbon', Carbon, 1998, **36**, 1309-1315.
[6] N.J. Welham, V. Berbenni, P.G. Chapman: 'Effect of Extended Ball Milling on Graphite', Journal of Alloys and Compounds, 2003, **349**, 255-263.
[7] A. Cuesta, P. Dhamelincourt, J. Laueyns, A. Martinez-Alonso and J. M. D. Tascon: 'Raman microprobe studies on carbon materials', Carbon, 1994, 32, 1523-1532.
[8] F. Tuinstra and J. L. Koening: 'Raman spectrum of graphite', J. Chem. Phys. 1970, **53**, 1126-1130.
[9] A. Denkevits, S. Dorofeev: "Dust Explosion Harzard in ITER", Fusion Eng. Des., 2005, **75-79**, 1135-1139.
[10] N.J. Welham, V. Berbenni and P.G. Chapman: 'Increased chemisorption onto activated carbon after ball-milling', Carbon, 2002, **40**, 2307-2315
[11] T. D. Shen, W. Q. Ge, K. Y. Wang, M. X. Quan, J. T. Wang, W. D. Wei and C. C. Koch: 'Structural disorder and phase transformation in graphite produced by ball milling' NanoStructured Materials, 1996, 8, 393-399.
[12] H. Wakayama, J. Mizuno, Y. Fukushima, K. Nagano, T. Fukunaga and U. Mizutani: 'Structural Defects in Mechanically Ground Graphite', Carbon, 1999, 37, 947-952.